Journal of Alloys and Compounds 812 (2020) 152163

Contents lists available at ScienceDirect

Journal of Alloys and Compounds

journal homepage: http://www.elsevier.com/locate/jalcom

Electrochemical reduction of nitric oxide in different carbon-driven solid state cells

Shuaini Wu [a], Wenyi Tan [a, *], Yu Peng [a], Jian Gao [a, c], Huangang Shi [a], Jifa Qu [a], Xiufang Zhu [b]

[a] Department of Environment Engineering, Nanjing Institute of Technology, Nanjing, 211167, Jiangsu, China
[b] Huaiyin Institute of Technology, Huaian, 223003, Jiangsu, China
[c] Beijing Technology and Business University, Beijing, 100048, China

ARTICLE INFO

Article history:
Received 9 July 2019
Received in revised form
1 September 2019
Accepted 4 September 2019
Available online 4 September 2019

Keywords:
Nitric oxides
Electrochemical reduction
Carbon
Solid state cell

ABSTRACT

A novelty of nitric oxide (NO) abatement technology in a solid state cell has been developed firstly, in which solid carbonaceous materials instead of gas (eg., H_2 or CH_4 etc.) work as reductant and fuel. The configuration of anode-supported nickel-yttrial stablized zirconia (Ni-YSZ), YSZ (yttrial stablized zirconia) electrolyte, LSM-YSZ (lanthanum strontium manganite-yttrial stablized zirconia) cathode, was fabricated into tubular cell with 13 mm in length and inner diameters 5 mm. Three carbonaceous materials, including activated carbon (AC), carbon black (BC) and graphite (GC), were investigated with regard to specific area, functional group, thermal activity and morphology by means of N_2-BET, FT-IR, TG and SEM, respectively. NO conversion efficiency in excess of 85% can be achieved in the solid state cells driven by AC at 800 °C, higher than cells by BC and GC. BC is one of cheaper carbonaceous material substituting for AC in NO electrochemical reduction, due to its comparable performance. Higher specific area (1745 $m^2 g^{-1}$) and higher content of oxygen-containing functional groups assigned to AC contributes to the better electrochemical behaviours evidenced by AC impedance spectra. Similar thermal activities can be observed both for AC and BC. This novel configuration offers a low-risk, inexpensive and highly-efficient option applicable to purification of exhausts from diesel or gasoline engine.

1. Introduction

The pollutants emitted by diesel engines or gasoline-driven cars, typically including nitrogen oxides (NO_x) and particulate matters (PM), have been causing severe environmental and human health problems. More and more stringent regulations have been established by many countries. Therefore, the emission control on vehicles has become one of critical issues in energy and environmental area.

The highly-efficient and low-cost technologies capable of reducing NO_x in exhausts from diesel engines or gasoline-driven cars have been focused intensively and widely. For example, NO_x storage-reduction catalyst (NSR) [1,2] and the ammonia/urea-SCR method have been developed for NO_x abatements for diesel engines [3], while three-way catalyst (TWC) for gasoline-driven cars on the intention of fuel economy. However, the environment requirements to be followed restrict the application of catalyst, whatever NSR catalysts or TWCs. NSR catalysts, typically like Pt/Ba/Al_2O_3, suitable for lean-burn conditions are easily susceptive towards sulfur in the level as low as 1 ppm, which is a great challenge for fuel quality [4]. The inability of TWCs to apply in lean-burn conditions is due to the strict compliance of A/F ratio (i.e., air to fuel is about 14.6) [1,5]. The ammonia/urea-SCR technology is currently put into practice for heavy-duty diesel, however, the disadvantage of this technology have been found in the fact that aqueous reductants, such as 32.5% wt/wt urea-solutions or aqueous ammonia, increase the transport and environment risks [6]. Additionally, many efforts have been put on the developments of non-ammonia reductants, vanadium-free catalysts as non-hazardous material and on improvements of urea injection system [7,8].

In recent decades, electrochemical reduction of NO in a solid state cell, consisting of solid oxide components (electrodes and electrolyte), becomes an attractive option, due to some advantages for this technology. For example, no reductant injection system, no adaptive control system for switching of lean and rich conditions

* Corresponding author.
E-mail address: twy1102@gmail.com (W. Tan).

https://doi.org/10.1016/j.jallcom.2019.152163
0925-8388/

and no noble metal catalysts are required, compared with SCR technology and NSR technology respectively. Further, other gas components (such as H_2O, CO_2, SO_2) and even products do not have negative effects on NO electrochemical reduction, because the configuration of device can separate exhaust from reactants by solid electrolyte, and only electrical current is produced [9]. Two types of electrochemical cell modes, the electrolysis cell mode (SOEC-NOx) and fuel cell mode (SOFC-NO_x) respectively, have been developed, since Pancharatnam et al. proposed firstly the idea of reducing NO_x electrochemically in solid state cell in 1970s [10]. In SOEC-NO_x mode, nitric oxides can be reduced via applying current with no reductant, based on oxygen-ion conductors (scandia stabilized zirconia, SSZ or yttrium stabilized zirconia, YSZ) and proton conductors ($SrCe_{0.95}Yb_{0.05}O_{3-\alpha}$) [11,12]. The drawback of SOEC-NOx is that the current efficiency is so low that almost 90% current are unavailable [13,14]. Low current efficiency for SOEC-NO_x is attributed to the preference of O_2 reduction on cathode [15]. On the other hand, SOFC-NO_x technology shows its unique merits, due to simultaneous NO reduction and electricity generation with the exhausts passing the cathode-side. A peak power density (PPD) of about 50 mW cm^{-2} was achieved by Huang et al. over Cu added LSCF-GDC cathode at 800 °C. Although serial of experiments were performed to discuss the effect of temperature, cathode composition, feed gas and external voltage on the electrical performance and NO conversion, the maximum PPD of about 80 mW cm^{-2} was achieved so far at 600–700 °C while NO conversion exceeds 78% at lower NO concentration mixed with O_2 feed [16,17]. Such low electrical performances mean nothing for application, let alone auxiliary equipments required for fuel or reductants (such as H_2, hydrocarbon etc).

In order to explore NO abatement in simple and high-efficient way, tubular solid state cells driven by three carbonaceous materials, including activated carbon (AC), carbon black (BC) and graphite (GC), were designed with the configuration of carbon-Ni-YSZ/YSZ/LSM for NO electrochemical reduction in this study. NO conversions in terms of carbonaceous materials were compared. The physical and chemical properties, eg., functional group, surface area, pore size and thermal activity of these carbonaceous materials were investigated, and electrochemical reduction process in NO atmosphere were interpreted by means of AC impedance spectra.

2. Material and methods

The anode-supported solid state cells consist of Ni-YSZ cermet anode, YSZ electrolyte and LSM cathode. YSZ powders purchased (Tosoφ) was mixed with a certain volume of ethylene glycol (EG) and then ultrasonically vibrated to obtain electrolyte precursor solution. Anode slurry were obtained by mixing the powders of 50:50 wt% YSZ and NiO (J.T. Baker) with organic solution, such as triethanolamine (TEA), Arabic gum (AG) etc, while cathode slurry was obtained by mixing LSM (purchased from CNITECH), with EG and glycerin. All slurries were ball-milled for 5 h then.

A 0.9 cm in diameter and 3.8 cm in length of tubular solid state cells driven by carbon were manufactured by slip-casting method. The detail procedure can be found in Ref. [18]. Briefly, after molding and afterwards removal from the mold, the sample was annealed at 950 °C for 3 h to obtain tubular Ni-YSZ substrate. Thin (~12 μm) dense YSZ electrolyte film was deposited by repeat-dipping of tubular substrate in YSZ electrolyte solution. The heat treatments of drying at 180 °C for 20 min and then sintering at 1400 °C for 5 h at least were followed. A LSM cathode layer was applied by slurry spray and then sintered at 950 °C for 2 h. Electrode surface was painted on by an amount of silver paste (DAD-87) and also wound by Ag wires for current passing. Fig. 1 demonstrates images of the protocol as well as its assembling. The apparent area of 6.0 cm^2 for

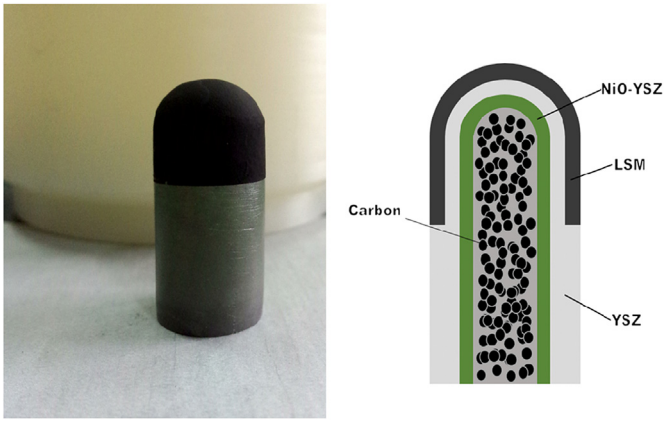

Fig. 1. The protocol of carbon-driven solid state cells for NO electrochemical reduction.

tubular cell was estimated according to the cell diameter.

After weighed about 1.0 g, three purchased carbonaceous materials, eg., GC (XFGNP, XFNANO INC), activated carbon (XFP01, XFNANO INC) and carbon black (Printex-U, Degussa), were filled into the anode chamber. A semitight method was applied for anode chamber. The filled carbon materials in anode chamber were then covered by asbestos and quartz sand to guarantee air outside separation from carbon and release of produced gas inside. NiO reduction before every experiment was performed through H_2 introduced into the carbon materials filled in tubular cell so as to reduce NiO into Ni.

Specific area and microstructure of solid carbonaceous materials were characterized by FT-IR and BET-N_2, respectively. NO conversion tests were performed in a custom-built apparatus. NO fed into cathode was balanced by helium gas and a concentration of 1560 ppm NO was measured by flue gas analyzer (Testo 350 Pro). NO conversion was measured when NO fed into cathode were at 50–150 ml/min [12].

$$\text{NO conversion } \% = (NO_{inlet}\text{-}NO_{outlet})/\ NO_{inlet} \times 100\%$$

Electrochemical impedance spectra were obtained at open circuit voltage (OCV) from 1 MHz to 10 mHz, with 12 points per decade (Versa STAT-4, Princeton Applied Research, USA). A thermogravimetric analyzer (NETZSCHSTA 449F3) was applied to evaluate thermal activity of solid carbonaceous materials from room temperature to 800 °C at a ramp rate of 10 °C/min with N_2 purging.

3. Results and discussion

3.1. Characterizations of solid carbonaceous materials

Fig. 2 shows the FT-IR spectra of three carbonaceous materials. The absorption bands of three carbonaceous materials are very similar, indicating that they contain the similar surface functional groups. A sharp absorption peak at 1380-1400 cm^{-1} observed in all samples indicates the presence of carboxyl-carbonate structures [19]. The bands at 1630 cm^{-1} with different relative intensity are ascribed to stretching vibration of double carbon bond in aromatic rings or C=O stretching vibration in carbonyls [20]. The broad bands ranging from 3100 to 3600 cm^{-1} correspond to the stretching O–H vibrations, which are resulted from the surface hydroxyl groups and physically absorbed water [19]. The difference of relative intensity at bands of 1380–1400 cm^{-1}, 1630 cm^{-1} and 3100-3600 cm^{-1} suggests that the AC and BC samples contain higher

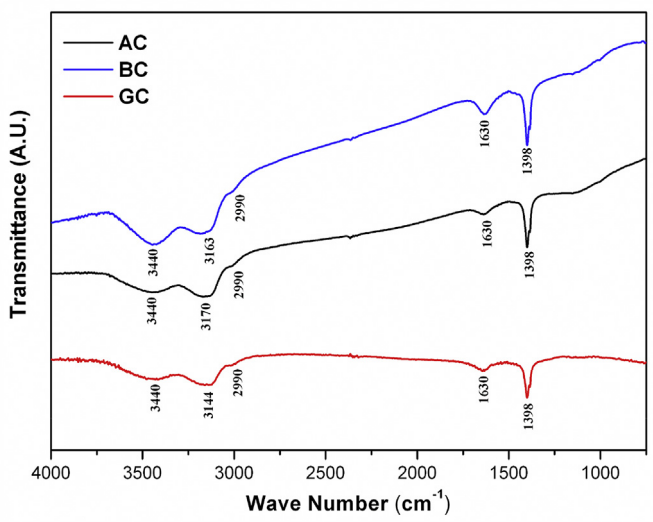

Fig. 2. FT-IR spectra of three carbonaceous materials.

content of oxygen-containing functional groups than GC sample does.

The N_2 physisorption was performed to obtain textural properties of all carbon samples. Their specific area, pore size distribution and pore volume calculated based on Barrett–Joyner–Halenda model were seen in Fig. 3 and Table 1.

According to the definition of IUPAC, the sorption isotherms of AC and BC samples seem to be typical type-IV isotherm with type-H3 hysteresis loops [21]. And the turning point of the N_2-adsorbed volume for AC and BC is 0.9, and the N_2 adsorbed volume further increases sharply under higher relative pressures. These features indicate that the mesopores are present in these two carbon samples but GC isn't [22]. Among the three carbon samples, AC has a significantly large BET surface area and the highest pore volume. A more than five-fold increase in BET surface area and one order of magnitude increase in pore volume for BC sample, compared to GC sample. Microstructure images observed by SEM as shown in Fig. 4 verify the results measured by BET-N_2. Lager surface area and mesopore structure favors electrochemically catalytic reaction of NO by providing more active sites and facilitating gas diffusion [23].

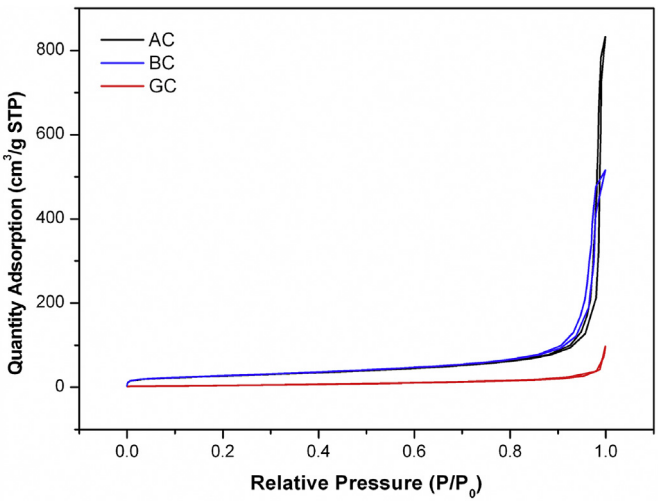

Fig. 3. N_2 adsorption-desorption isotherms of three carbonaceous materials.

3.2. NO conversion in different solid carbonaceous materials

The performance comparison of NO electrochemical reduction by three solid carbonaceous materials is given in Fig. 5.

Significant difference of conversion performances can be observed, when 1560 ppm NO was introduced into cathode chambers. The best performance of NO conversion of 86.22% is obtained for AC at 800 °C. Meanwhile, a current density of 52 mA cm^{-2} was achieved. Huang et al. applied pure H_2 as fuel to reduce 150–5000 ppm NO at 800 °C in planar electrochemical cells, which worked in SOFC-NOx mode as above mentioned. Besides 78% NO conversion achieved, endogenous potential difference was produced due to oxygen partial pressure between anode and cathode, and a current density of 220 mA cm^{-2} was generated in closed circuit [16]. In our present study, solid carbon replaces gaseous H_2 to form endogenous potential difference, promoting NO electrochemical reduction without auxiliary reductant supply system or external current applied. NO conversion and current density in case of BC are 68.22% and 34 mA cm^{-2}, a little lower than those of AC, but still acceptable when considering their different costs. The worst conversion performance is achieved for GC, less than half of performance for AC. It is more clearly found that NO conversion in case of AC and BC samples both decrease gradually with reaction time. Within 140 min, NO conversion performance reduces from 86.22% to 80.04% for AC, and from 68.22% to 63.83% for BC. No obvious decline of performance is found in case of GC. Difference in NO conversion is attributed to the different carbon materials participating in electrochemical reaction. Similar to direct carbon fuel cell (DCFC), carbon material filled in anode chamber is consumed by means of oxidation by oxygen ions (O^{2-}) from the cathode [24]. The oxygen ions (O^{2-}) in DCFC are originated from pure oxygen or oxygen in air. When NO gas was fed into cathode instead of oxygen, oxygen ions are only originated from NO decomposition and then transport across the solid electrolyte to participate the carbon oxidation in anode. The decreasing performances also indicate the active oxygen species taking part in the electrochemical reactions are decreasing.

According to the previous literature [25], the way that carbon materials participating in the electrochemical oxidation includes three reactions as follows [25],

$$C + O^{2-} = CO + 2e^- \quad (1)$$

$$C + 2O^{2-} = CO_2 + 4e^- \quad (2)$$

$$CO + O^{2-} = CO_2 + 2e^- \quad (3)$$

Reaction (1) and (2) is the direct electrochemical oxidation of solid carbon as active species, while reaction (3) is oxidation of CO as incomplete oxidation product. Limited by triple phase boundary (TPB) region in gas-solid reaction, NO electrochemical reduction are not pushed ahead by reaction (1) and (2). Since atmosphere air present in chamber would then react with carbon materials in reduced atmosphere, CO_2 would be formed consequently. According to reverse Boudouard reaction (4),

$$C + CO_2 = CO \quad (4)$$

Gaseous CO produced in-situ tends to facilitate NO electrochemical reduction due to CO high diffusivity as reaction (3) presents. CO plays a critical role in reducing NO electrochemically. The semitight method applied for anode chamber as described in experiment section aimed to facilitate reverse Boudouard reaction. As oxygen partial pressure in anode chamber decreases, due to oxidation of carbon materials, atmosphere O_2 diffuses into the

Table 1
Textural properties of carbonaceous materials.

Samples	BET surface area (m^2/g)	Pore volume (cm^3/g)	Average pore diameter (nm)
AC	1745	1.12	2.02
BC	95.57	1.29	26.96
GC	18.98	0.15	15.84

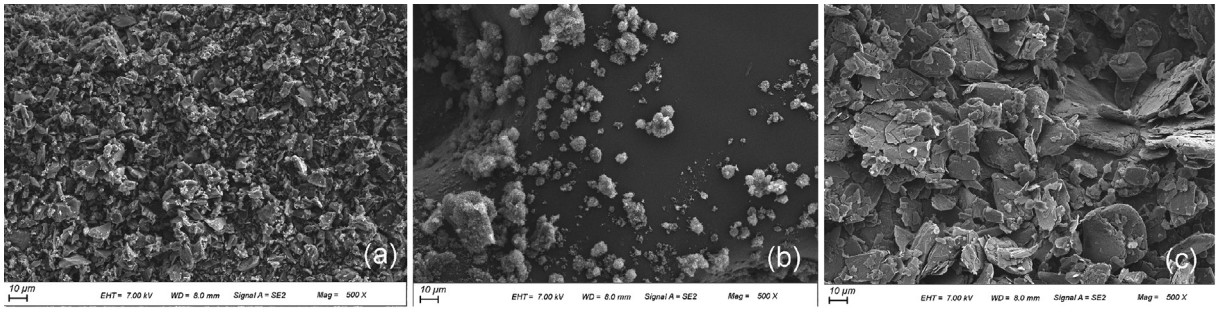

Fig. 4. SEM images of carbonaceous materials: (a) AC; (B) BC; (c) GC.

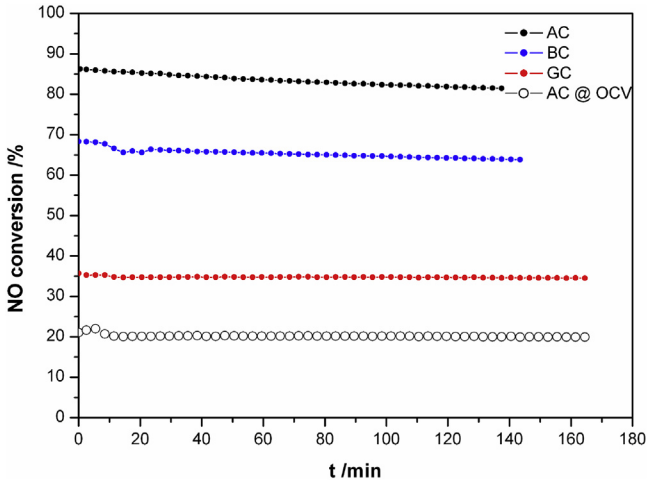

Fig. 5. Variations of NO conversion as a function of operation time.

(NO conversion under OCV condition is presented only in case of AC, due to be independent of carbon materials)

chamber through the channels of the filled asbestos and quartz sand. CO_2 can be produced continuously, and thereby CO is produced in reducing atmosphere inside when solid carbon is sufficient. In order to verify the carbon's role in electrochemical reduction of NO, the mass of AC and GC remained after 60 min and 140 min were weighted respectively under closed-circuit conditions. As a result, about 24% and 78% in mass loss of AC can be observed after 60 min and 140 min, while no obvious mass loss for GC takes place. Compared to GC, AC tends to follow Boudouard reaction more easily. Mass loss in case of AC is responsible for electrochemical reduction of NO, and that lower NO conversion is attributed to inactive GC. Considering the carbon loss, a system for carbon refilling referred to that of DCFCcan be considered [26].

NO conversion under OCV condition for three carbon materials was measured. It is noted that NO conversions are independent of carbon materials, and NO conversion rate of 21% are achieved without carbon loss, in spite of low conversion. Self-decomposition of NO over LSM at 800 °C and the electrochemical promotion of catalysis under OCV condition contribute to the conversion [16,27]. Such low NO conversion is related to the lower OCV as Table 2 shows. If OCV was increased highly enough, it is anticipated that NO can be reduced electrochemically without any carbon loss. Enhanced NO conversion from 21% to 85% above (in case of AC) is exactly due to the current produced under closed-circuit condition. The significant difference in NO conversion shows the electrochemical reactions play an important role in NO abatement.

3.3. Electrochemical properties in different solid carbonaceous materials

Another evidence that NO electrochemical reduction is caused by carbon filled in anode is their electric performances (eg., open circuit voltage, etc) and their electrochemical properties. Table 2 lists the OCV values at 800 °C when air and NO were fed into cathode, respectively, in which two flows rates of NO was conducted. OCV values in NO atmosphere are around 0.1 V, one-tenth of that in air. Despite much lower OCV values achieved in NO flow than in air flow, OCV values vary with flow rates of gas into cathode. According to Nernst equation, OCV is proportional to logarithm of the ratio of partial pressure of CO to CO_2 ($\ln\frac{p_{CO}p_{O_2}^{\frac{1}{2}}}{p_{CO_2}}$), or to logarithm of the ratio of partial pressure of O_2 to CO_2 ($\ln\frac{p_{O_2}}{p_{CO_2}}$), when active species of carbon are CO and solid carbon, respectively [28,29]. Unlike DCFC in air, oxygen in the process of NO electrochemical reduction driven by carbon is originated from NO decomposition, and consequently the low oxygen partial pressure (p_{O2}) contributes to the low OCV. An increase in flow rates of gas (eg., air and NO) produces a higher oxygen partial pressure (p_{O2}) and thereby enhances the OCV.

The electrochemical behaviors for NO reduction can be recorded in AC impedance spectra as illustrated in Fig. 6. The AC impedance spectra for three carbonaceous materials consist of typical semicircles measured in high frequency and low frequency. The

Table 2
OCV (v) at 800 °C under different flow rates of air and NO fed into cathode.

Operation conditions	AC		BC		GC	
	in air	in NO	in air	in NO	in air	in NO
50 ml/min	0.92	0.082	0.90	0.094	0.90	0.088
150 ml/min	1.01	0.12	1.14	0.15	0.94	0.098

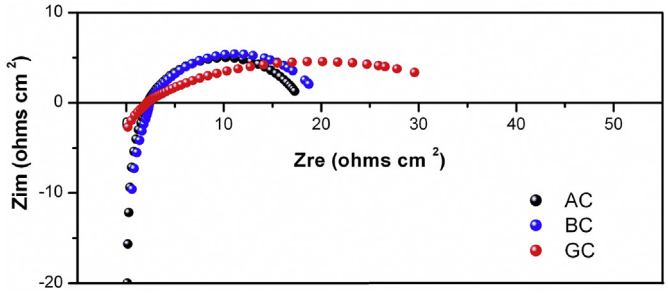

Fig. 6. AC impedance spectra during electrochemical reduction of NO in solid state cells.

intercept of semicircle on the real axis in high frequency represents ohmic resistance (R_s), most of which is attributed to resistance of electrolyte, electrode and their contact resistance. The intercept difference on the real axis between high and low frequency corresponds to the polarization resistance (R_p), which includes series of electrochemical reactions taking place both at anode and cathode. It is found that ohmic resistances (R_s) for cells driven by three carbonaceous materials are all around 2 Ω cm^2, even in the process of electrochemical reduction of NO. Significant difference is observed in the polarization resistance (R_p). The cell driven by GC has the highest value of R_p, more than 30 Ω cm^2, and the R_p values for cells driven by BC and AC are 20 Ω cm^2 and 18 Ω cm^2, respectively. Considering the same NO atmosphere in cathode and the configuration of cells, the difference for R_p values is attributed to the different activities of carbonaceous materials applied.

Fig. 7 presents the TGA curves for three carbonaceous materials in N_2 purge gas in temperature range of 20–800 °C. The rates of weight loss in TGA profiles provide an indicator of carbonaceous materials' reactivity, which is associated with their activity for chemical and electrochemical reactions [30]. There are two significant decline of weight taking place during temperature-rise period. (1) Weight losses for AC and BC before 100 °C correspond to the release of the moisture content; (2) As the temperature rises from 100 to 600 °C, slight weight losses for all samples are ascribed to slow release of volatile components [31,32]; (3) AC and BC undergoes similar weight loss in inert gas. Apparent declines in weight after 600 °C occur continuously for AC and BC, and it is a clue that AC and BC have higher thermal reactivity due to the decomposition of volatiles and surface functional group [33]. FTIR spectra in Fig. 2 also verify the presence of higher content of oxygen-containing functional groups. Higher activity of carbonaceous material favors mass or charge transfer during electrochemical reactions, and therefore contributes to lower R_p values in AC impedance spectra [34]. In spite of similar thermal reactivity for AC and BC samples, superior surface area and pore volume in case of AC in Table 1 also favors mass transfer and gas diffusion. The activity orders obtained in TGA profile are in accordance with the electrochemical performances of cells.

For comparison, electric performances of solid state cells driven by different carbonaceous material in air are shown in Fig. 8 as typical I–V and I–P polarization curves, when the solid state cells work in DCFC mode. The maximum power densities (MPD) achieved at 800 °C in DCFCs driven by AC, BC and GC are 185 mW cm^{-2}, 148 mW cm^{-2} and 74 mW cm^{-2}, respectively. DCFCs with planar structure built by John T.S. Irvine's group followed the same orders of electric performances, when AC, BC and GC were applied as fuel [35]. The electric performances of DCFCs are also heavily dependent of carbonaceous materials, although more distinct differences of electric performances are present in DCFC mode.

In order to understand the electrochemical behaviors of cells in different atmospheres, AC impedance spectra for cells with the same configuration in air and NO atmosphere are compared in Fig. 9. As mentioned above, the cell in air atmosphere is assigned to DCFC mode, while that in NO atmosphere is de-NOx mode. The ohmic resistance ($R_{s,air}$) and polarization resistance ($R_{p,air}$) in DCFC mode are 1.97 and 2.22 Ω cm^2, while ohmic resistance ($R_{s,NO}$) and polarization resistance ($R_{p,NO}$) in de-NOx mode are 2.24 and 18 Ω cm^2. Ohmic resistance in DCFC mode decreases very slightly in comparison with that in de-NOx mode. However, polarization resistance increases greatly. Unlike the spectrum recorded in de-NOx mode that two semicircles are merged together, two semicircles can be distinguished clearly in DCFC mode. The characteristic of impedance spectra suggests that the lower oxygen partial pressure in NO atmosphere than air causes to the inferior transport ability of oxygen ion in electrolyte, and meanwhile it contributes to the deterioration in charge transfer processes and gas diffusion processes [36].

4. Conclusion

Electrochemical reduction of NO without injecting liquid reductant can be realized effectively in a solid state cell, when solid carbonaceous materials, such as activated carbon (AC), black carbon

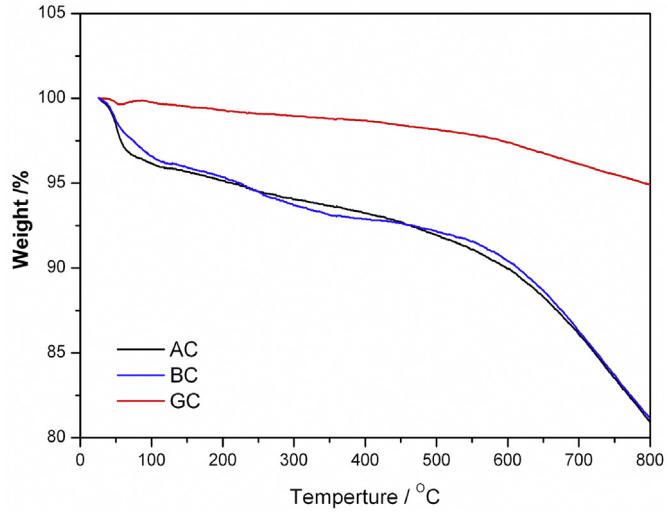

Fig. 7. TGA profiles for three carbonaceous materials in N_2 atmosphere.

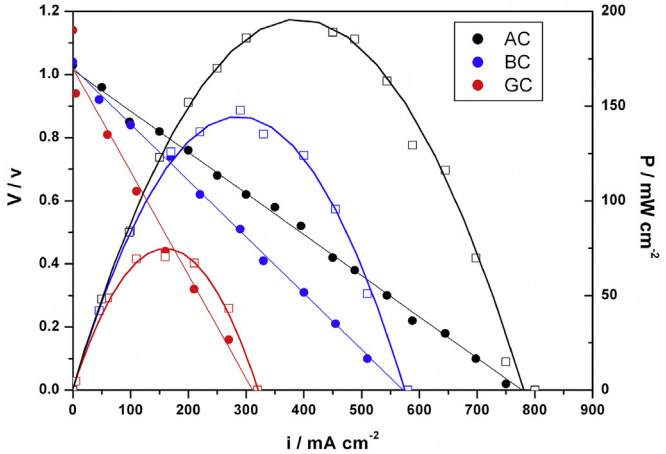

Fig. 8. Polarization curves of solid state cells in DCFC mode.

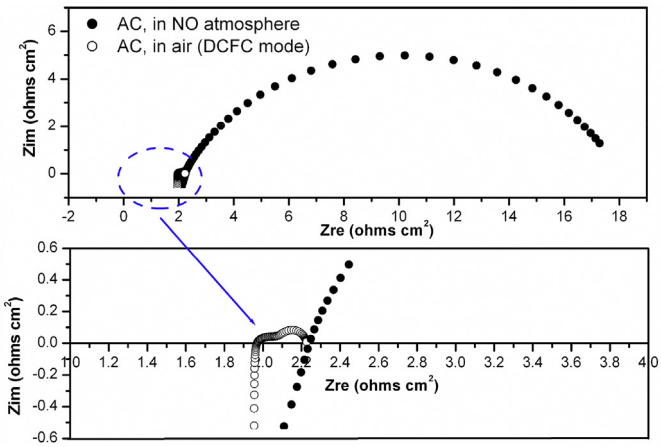

Fig. 9. Comparison of AC impedance spectra of solid state cells driven by activated carbon in different modes.

(BC) and graphite (GC), were filled into tubular cell. At 800 °C, the cell driven by AC is able to reduce NO electrochemically as highly as 86.22%. The NO conversions for BC and GC are respectively 68.22% and 35.65%, and BC can replace AC to some degree. Better NO conversion and superior electrochemical behavior for cell driven by AC are attributed to higher specific area, higher content of oxygen-containing functional groups and thermal activity of AC.

Acknowledgments

The authors acknowledge the financial support from the National Natural Science Foundation of China (No. 51678291), the Six Top Talents Plan in Jiangsu Province (No. JNHB-029) and the Natural Science Foundation of Jiangsu Province (Grant No. BK20160425). Miss Wu also appreciates the Jiangsu Students' Platform for innovation and entrepreneurship training program (No. 201711276001Z).

References

[1] Si Matsumoto, Recent advances in automobile exhaust catalysts, Catal. Today 90 (2004) 183–190.
[2] S. Roy, M.S. Hegde, G. Madras, Catalysis for NOx abatement, Appl. Energy 86 (2009) 2283–2297.
[3] V. Praveena, M.L.J. Martin, A review on various after treatment techniques to reduce NOx emissions in a CI engine, J. Energy Inst. 91 (2018) 704–720.
[4] J.-J. He, M. Meng, Z.-Q. Zou, X.-X. He, High-temperature NOxStorage and sulfur-resistance of the lithium-based lean-burn NOxTrap catalyst Pt/Li/TiO2–Al2O3, Catal. Lett. 136 (2010) 234–242.
[5] J. Wang, H. Chen, Z. Hu, M. Yao, Y. Li, A review on the Pd-based three-way catalyst, Catal. Rev. 57 (2015) 79–144.
[6] M. Koebel, M. Elsener, M. Kleemann, Urea-SCR: a promising technique to reduce NOx emissions from automotive diesel engines, Catal. Today 59 (2000) 335–345.
[7] A.W.-L. Ting, M.P. Harold, V. Balakotaiah, Elucidating the mechanism of fast cycling NOx storage and reduction using C3H6 and H2 as reductants, Chem. Eng. Sci. 189 (2018) 413–421.
[8] B. Guan, R. Zhan, H. Lin, Z. Huang, Review of state of the art technologies of selective catalytic reduction of NOx from diesel engine exhaust, Appl. Therm. Eng. 66 (2014) 395–414.
[9] T.-J. Huang, C.-Y. Wu, D.-Y. Chiang, Effect of H2O and CO2 on NOx emission control for lean-burn engines by electrochemical-catalytic cells, J. Ind. Eng. Chem. 19 (2013) 1024–1030.
[10] S. Pancharatnam, R.A. Huggins, D.M. Mason, Catalytic decomposition of nitric oxide on zirconia by electrolytic removal of oxygen, J. Electrochem. Soc. 122 (1975) 869–875.
[11] K.K. Kalimeri, C.I. Athanasiou, G.E. Marnellos, Electro-reduction of nitrogen oxides using steam electrolysis in a proton conducting solid electrolyte membrane reactor (H+-SEMR), Solid State Ion. 181 (2010) 223–229.
[12] T. Hibino, T. Inoue, M. Sano, Electrochemical reduction of NO by alternating current electrolysis using yttria-stabilized zirconia as the solid electrolyte: Part II. Modification of Pd electrode by coating with Rh, Solid State Ion. 130 (2000) 31–39.
[13] H. Kamata, K. Takahashi, Odenbrand CUI. The role of K2O in the selective reduction of NO with NH3 over a V2O5(WO3)/TiO2 commercial selective catalytic reduction catalyst, J. Mol. Catal. A Chem. 139 (1999) 189–198.
[14] K. Kammer, Electrochemical DeNOx in solid electrolyte cells—an overview, Appl. Catal. B Environ. 58 (2005) 33–39.
[15] J. Shao, Y. Tao, K.K. Hansen, Highly selective NOx reduction for diesel engine exhaust via an electrochemical system, Electrochem. Commun. 72 (2016) 36–40.
[16] T.-J. Huang, C.-Y. Wu, C.-C. Wu, Effect of temperature and concentration on treating NO in simulated diesel exhaust via SOFCs with Cu-added (LaSr)MnO3 cathode, Chem. Eng. J. 168 (2011) 672–677.
[17] T.-J. Huang, C.-Y. Wu, C.-C. Wu, Simultaneous CO and NOx removal from simulated lean-burn engine exhaust via solid oxide fuel cell with La0.8Sr0.2Mn0.95Cu0.05O3 cathode, Electrochem. Commun. 13 (2011) 755–758.
[18] B. Yang, R. Ran, Y. Zhong, C. Su, M.O. Tadé, Z. Shao, A carbon–air battery for high power generation, Angew. Chem. 127 (2015) 3793–3796.
[19] C. J Paul, W. Shunnian, Acid/Base-treated activated carbons: characterization of functional groups and metal adsorptive properties, Langmuir the Acs Journal of Surfaces & Colloids 20 (2004) 2233–2242.
[20] F. Abild-Pedersen, J. Greeley, F. Studt, J. Rossmeisl, T.R. Munter, P.G. Moses, E. Skúlason, T. Bligaard, J.K. Nørskov, Phys. Rev. Lett. 99 (2007) 16105.
[21] Barry Crittenden WJT, Adsorption Technology and Design, first ed., Elsevier Science & Technology, 1998, p. 288.
[22] X. Wang, W. Wen, J. Mi, X. Li, R. Wang, The ordered mesoporous transition metal oxides for selective catalytic reduction of NOx at low temperature, Appl. Catal. B Environ. 176–177 (2015) 454–463.
[23] Y. Li, Y. Li, Y. Wan, S. Zhan, Q. Guan, Y. Tian, Structure–performance relationships of MnO2 nanocatalyst for the low-temperature SCR removal of NOX under ammonia, RSC Adv. 6 (2016) 54926–54937.
[24] C. Jiang, J. Ma, G. Corre, S.L. Jain, J.T.S. Irvine, Challenges in developing direct carbon fuel cells, Chem. Soc. Rev. 46 (2017) 2889–2912.
[25] S. Hasegawa, M. Ihara, Reaction mechanism of solid carbon fuel in rechargeable direct carbon SOFCs with methane for charging, J. Electrochem. Soc. 155 (2008) B58–B63.
[26] S.A.A. Naqvi, M.T. Mehran, R.-H. Song, J.-W. Lee, S.-B. Lee, S.-J. Park, D.-R. Shin, T.-H. Lim, Performance evaluation of solid oxide carbon fuel cells operating on steam gasified carbon fuels, Chem. Eng. J. 300 (2016) 384–393.
[27] H.J. Hwang, J.-W. Moon, M. Awano, Microstructure and NO decomposition behavior of sol–gel derived (La0.8Sr0.2)0.95MnO3/yttria-stabilized zirconia nanocomposite thin film, Mater. Res. Bull. 38 (2003) 311–318.
[28] L. Zhang, J. Xiao, Y. Xie, Y. Tang, J. Liu, M. Liu, Behavior of strontium- and magnesium-doped gallate electrolyte in direct carbon solid oxide fuel cells, J. Alloy. Comp. 608 (2014) 272–277.
[29] N. Nakagawa, M. Ishida, Performance of an internal direct-oxidation carbon fuel cell and its evaluation by graphic exergy analysis, Ind. Eng. Chem. Res. 27 (1988) 1181–1185.
[30] A. Fuente-Cuesta, C. Jiang, A. Arenillas, J.T.S. Irvine, Role of coal characteristics in the electrochemical behaviour of hybrid direct carbon fuel cells, Energy Environ. Sci. 9 (2016) 2868–2880.
[31] L. Fan, J. Wang, L. Zhao, N. Hou, T. Gan, X. Yao, P. Li, Y. Zhao, Y. Li, Effects of surface modification on the reactivity of activated carbon in direct carbon fuel cells, Electrochim. Acta 284 (2018) 630–638.
[32] S.L. Jain, J. Barry Lakeman, K.D. Pointon, R. Marshall, J.T.S. Irvine, Electrochemical performance of a hybrid direct carbon fuel cell powered by pyrolysed MDF, Energy Environ. Sci. 2 (2009) 687–693.
[33] M. Konsolakis, N. Kaklidis, V. Kyriakou, I. Garagounis, T. Kraia, A. Arenillas, J.A. Menéndez, R. Strandbakke, G.E. Marnellos, The combined impact of carbon type and catalyst-aided gasification process on the performance of a Direct Carbon Solid Oxide Fuel Cell, Solid State Ion. 317 (2018) 268–275.
[34] S. Jiang, Development of lanthanum strontium manganite perovskite cathode materials of solid oxide fuel cells: a review, J. Mater. Sci. 43 (2008) 6799–6833.
[35] S. Li, W. Pan, S. Wang, X. Meng, C. Jiang, J.T.S. Irvine, Electrochemical performance of different carbon fuels on a hybrid direct carbon fuel cell, Int. J. Hydrogen Energy 42 (2017) 16279–16287.
[36] F. Yen-Pei, Sm0.5Sr0.5Co0.4Ni0.6O3−δ–Sm0.2Ce0.8O1.9 as a potential cathode for intermediate-temperature solid oxide fuel cells, Int. J. Hydrogen Energy 35 (2010) 8663–8669.